A Measurement Of Muon Fluences Associated With the Fermilab Proton Center Charged Hyperon Beam

Joseph Lach, Li Yun Shan*
Fermilab
February 21, 1989

Introduction. The Fermilab Proton Center (PC) hyperon beam was commissioned in the spring of 1980 and first used by E497 to measure charged hyperon fluxes, polarization and magnetic moments. It has subsequently been used for a number of other experiments requiring beams of charged and neutral hyperons, neutral kaons and neutrons. However, a systematic measurement of muon fluence associated with the beam particles has not been done. This note describes an attempt to do so during the recent run of E756 in the winter of 1987/88. These measurements were done parasitically to the E756 running so that the choice of targets or beam conditions was not always optimal for a systematic study.

It is hoped that these measurements will be useful in the estimation of backgrounds for PC experiments as well as for the design of future hyperon beams.

Beam and Area. Figure 1 shows a plan view of the area including the experimental enclosure and magnet locations. The experimental enclosure, designated PC4 in the standard Fermilab notation, is below grade level. The beam line was horizontal and centered 4.0 feet above the floor of PC4. Note that the counting areas (Portakamps) which housed much of the electronic equipment and computers associated with these experiments is at grade level. The difference in elevation between the beam and the floor of the Portakamps (Figure 1) was about 14 feet.

For these measurements the 800 GeV primary proton beam was allowed to impinge either on a 3.6 inch long Be target (20% of an interaction length) or a 6.0 inch long Cu target (one interaction length) located at the entrance of the hyperon magnet (Figure 1). This magnet is described in detail in references 2 and 5. The forward produced secondary particles are collimated and transported by the hyperon magnet. The hyperon magnet provides momentum analysis for the transmitted particles and also contains the primary beam dump. The charged particle rates outside of the beam were not significantly effected by the length or composition of the target. However, the choice of target material did effect the secondary particle rates in the beam. Since we will only be concerned with the rates outside of the beam we will ignore these target differences and combine the data from the two targets.

The production angle of the secondary particles can be controlled by changing the incident angle of the 800 GeV primary proton beam. Thus the production angle of the beam emerging from the hyperon magnet could be varied from approximately -3 to +3 mrad in either the vertical or horizontal direction by changing the direction of the incident proton beam. The geometry of the hyperon collimator, which is imbedded in the hyperon magnet, is shown in Figure 2. Note that it is **not** the same as that described in references 2 and 5. This collimator can be easily replaced and is usually tailored to the individual experiment. The magnetic field in the hyperon magnet is in the vertical direction and can be as large as 35.7 kG with a current of 3600 Amps. Figure 3 shows the relationship of magnet current to the magnetic field.

Not shown in Figure 1 is the iron and concrete shielding which was place on the top and sides of the hyperon magnet.

Coordinates. The coordinate system used for the measurements has its origin at the exit of the hyperon magnet channel. The z-axis is in the direction of the nominal beam center line. The positive y-axis is vertical (up) and the x-axis is such as to make a right handed system. Data was collected with reference to this system (Figure 1). The muon telescope was moved along a number of lines (A-F) and a set of points in the Portakamps. The data recorded at a set of points on each of these lines form the basis of our muon fluence measurements.

The Flux Measurements. The flux was measured using a simple muon telescope consisting of a pair of plastic scintillation counters. These counters had dimensions $25.5\times33.5\times0.3$ cm^3 and $10.6\times10.16\times0.16$ cm^3. The counters were overlapped and separated by 7.0 cm; an electronic coincidence was required between them. Thus the effective area of the coincidence signal was determined by the area of the smaller counter. The sizes of these counters was such that they had little directional discrimination. For these measurements they were oriented so that they exhibited their maximum area to the direction of the target.

The accelerator was operated with a full cycle of 57 s and the beam extracted and brought onto our target for a time of 23 s. Standard electronic modules were used to make the coincidence between the two counters and both the singles and coincidence rates were recorded. Except in the small region of the secondary beam itself, this coincidence rate is dominated by muons since the particles would have had to traverse at least 7 m of shielding. Inserting a few cm of lead between the counters did not appreciably effect the coincidence rate and reinforced this assumption.

Also available was a measurement of the beam flux exiting the hyperon channel (Figure 2). This coincidence signal originated from a set of 4 small scintillation counters which just covered the spatial extent of the beam. It was provided by the E756 experimenters and designated PC4SCPI. The proton beam flux incident on the target was recorded by a secondary emission monitor (PC3SEM) located upstream of the target. All of the above information as well as relevant magnet currents were recorded for each accelerator cycle on the beam line control computer and could then be displayed. A typical measurement required only one beam pulse.

A set of measurements consisted of moving the muon telescope systematically along a given direction. We describe each of the passes in Table 1 and they are shown on Figure 1. They consisted of a set of passes done in the x-direction in PC4 and a set of passes done at grade level. For all of the passes done in PC4, (passes C-F), the muon telescope was centered at beam height ($y=0$). The grade level passes were at the beginning (pass B) and end (pass A) of the hyperon extension (Figure 1). The final grade level pass was done inside the Portakamps and is called pass Pk.

The muon fluence per incident proton is a function of the current in the hyperon magnet (PC3ANA in the standard nomenclature) as well as its polarity and the targeting angle. The polarity convention is such that the sign of the charged beam transported by the hyperon magnet channel is the same as the sign of the magnet current. The current determined the momenta of the particles. In terms of the muon fluence, which originated both from interactions in the target and the beam dump, a larger magnetic field deflected muons further away from the beam. Measurements were taken at various values of magnetic field and polarity. All measurements were taken at forward production angles (zero degree production). However, other measurements not reported here, indicate that if production angles are varied within a few mrad, the muon fluence is not significantly changed, although the charged particle flux through the hyperon channel will exhibit the expected fall off with transverse momentum. This picture is consistent with the muon fluence depending on the number of incident protons but independent of whether they interact in the target, or the near-by beam dump.

For each point measured, the muon fluence (muons/cm^2/incident proton) was computed from the recorded muon telescope coincidence rate, the PC3SEM, the known counter area, and the 23 s beam spill time. These were then plotted for each pass as indicated in Table 1.

Discussion. Figure 4 shows the muon fluence in the counting area of E715/E761. This is a region that will be occupied by the experimenters when the beam is operational. The curve in this plot, as in the others, is drawn merely to guide the eye. A radiation dose of 1.0 mrem is equivalent to a muon fluence of 25,000 muons/cm^2. An area with no occupancy limit[6] should be < 0.25 mrem/hour. With the normal Fermilab Tevatron repetition rate of one pulse per minute, this would allow us to run comfortably with $\approx 5\times10^{11}$ protons per pulse incident on our target.

Figures 5 and 6 are rates at grade level above the underground experimental enclosure. These are areas which are accessible when the beam is operational but are of minimal occupancy.

Figures 7 to 10 display the particle fluences at beam height as a function of x for various z positions. Note the logarithmic vertical scale. In these passes the muon telescope was moved through the beam. Thus the charged particle flux peak in these plots near x=0, is due almost entirely to charged beam particles (**not** muons) which come through the beam channel. For measurements outside of the charged particle beam the flux is due to muons. This was confirmed using the concomitant measurement of the beam rate signal (PC4SCPI) mentioned previously and provided by E756.

Some general features should be noted. As the magnet current is increased, the muon fluences outside of the hyperon beam decrease. This is most clearly seen in Figure 7 where three magnet currents are plotted. As expected the muon fluence also decreases as one moves to larger z.

I would like to thank the members of E756, the Research Division Operations Department, and the Research Division Radiation Safety Group for their cooperation in the data taking.

This work was supported by the U.S. DOE under contract #DE-AC02-76CH03000

*Visitor from Institute Of High Energy Physics, Beijing, China

1. C. Ankenbrandt et al, Phys. Rev. Lett. 51, 863 (1983)
2. T. R. Cardello et al, Phys. Rev. 32, 1 (1985)
3. Y. W. Wah et al, Phys Rev. Lett 55, 2551 (1985)
4. J. L. Thron et al, Phys, Rev. 31D 451 (1985)
5. T. R. Cardello, Fermilab TM-964 (March 1980)
6. Fermilab Radiation Guide, March 1988.

Table 1
All data in feet

Pass	x	y	z	Figure
Pk	37.6	17.5	252.3 to 392.25	4
A	-17.5 to +27.5	15.9	279.5	5
B	-23.0 to 22.0	15.9	160.0	6
C	-8.0 to 3.0	.0	37.4	7
D	-9.0 to 9.0	.0	76.0	8
E	-5.0 to 3.0	.0	163.1	9
F	-5.0 to 1.0	.0	212.9	10

Figure 1

Proton Center Plan View

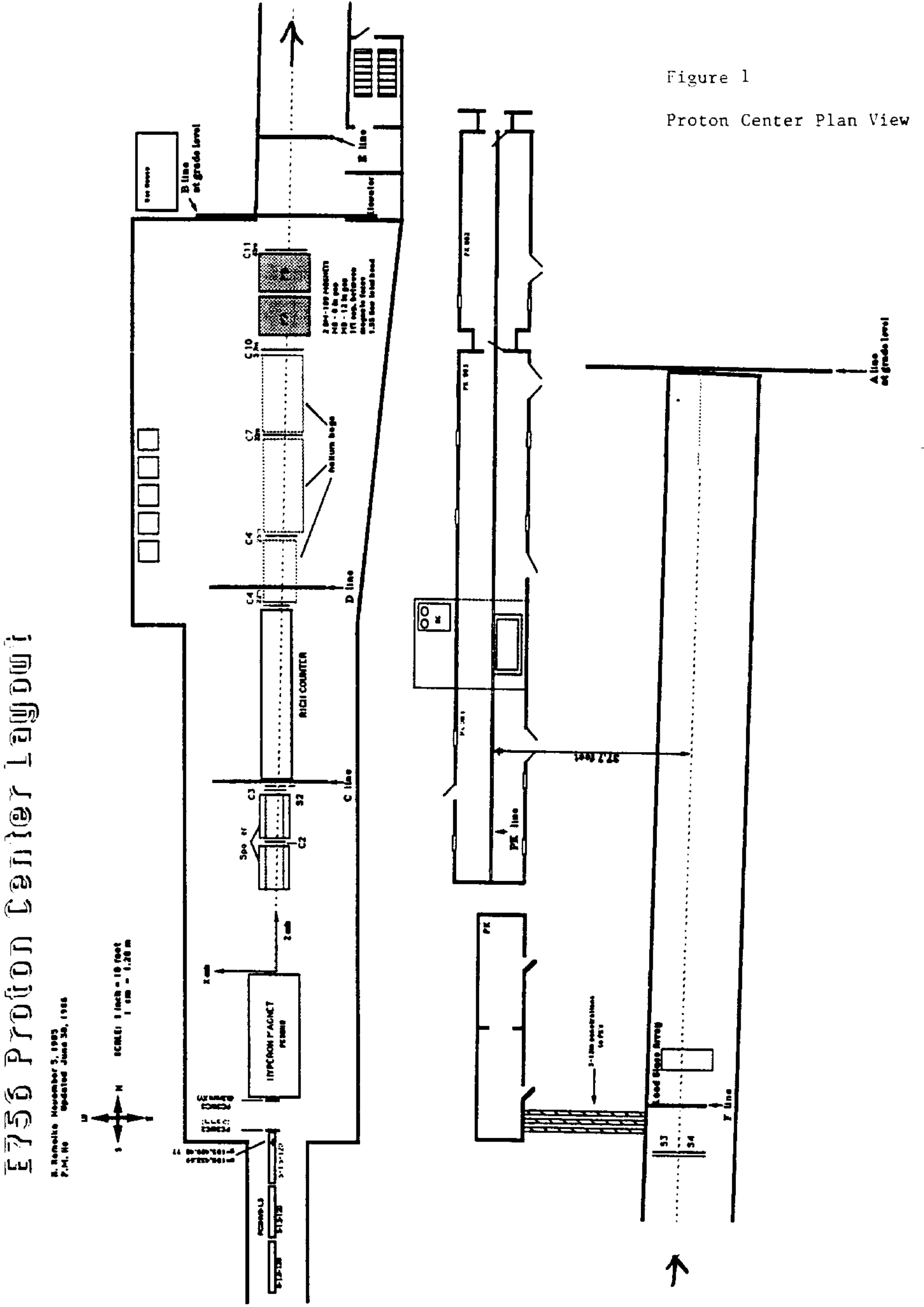

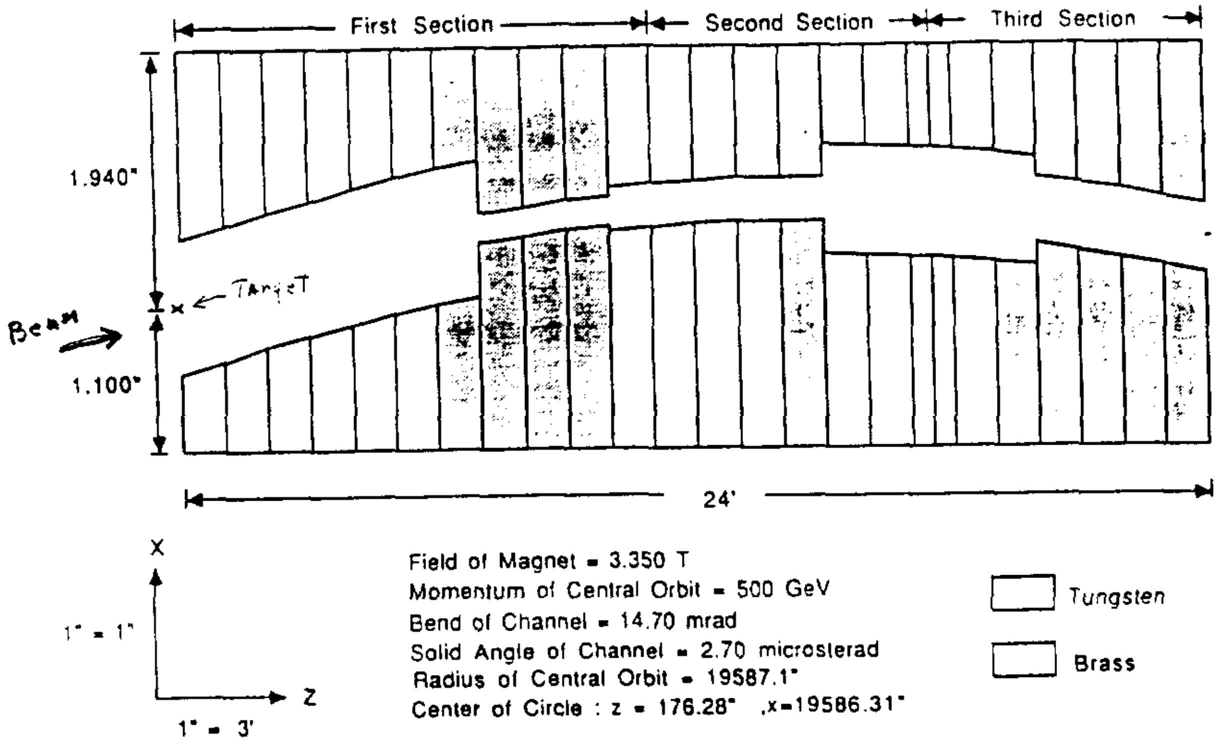

Bend View of E756 Collimator

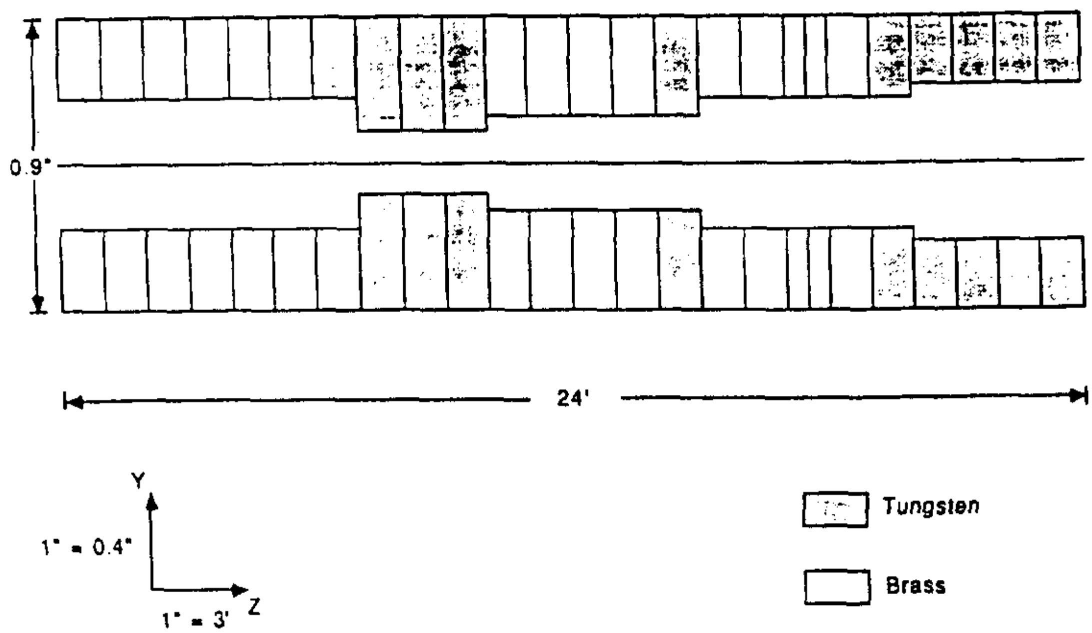

Non-Bend View of E756 Collimator

Figure 2 E756 Collimator

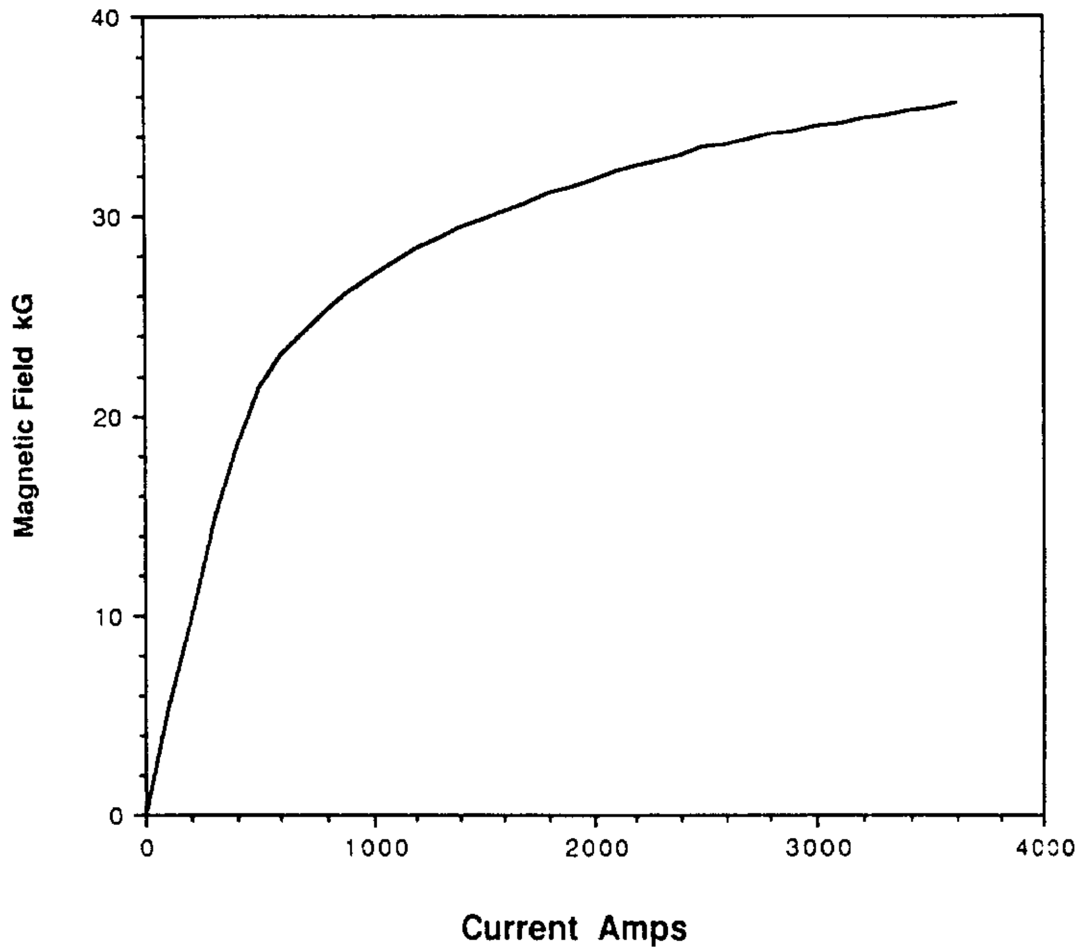

Figure 3 Magnetic Field vs Current in Hyperon Magnet

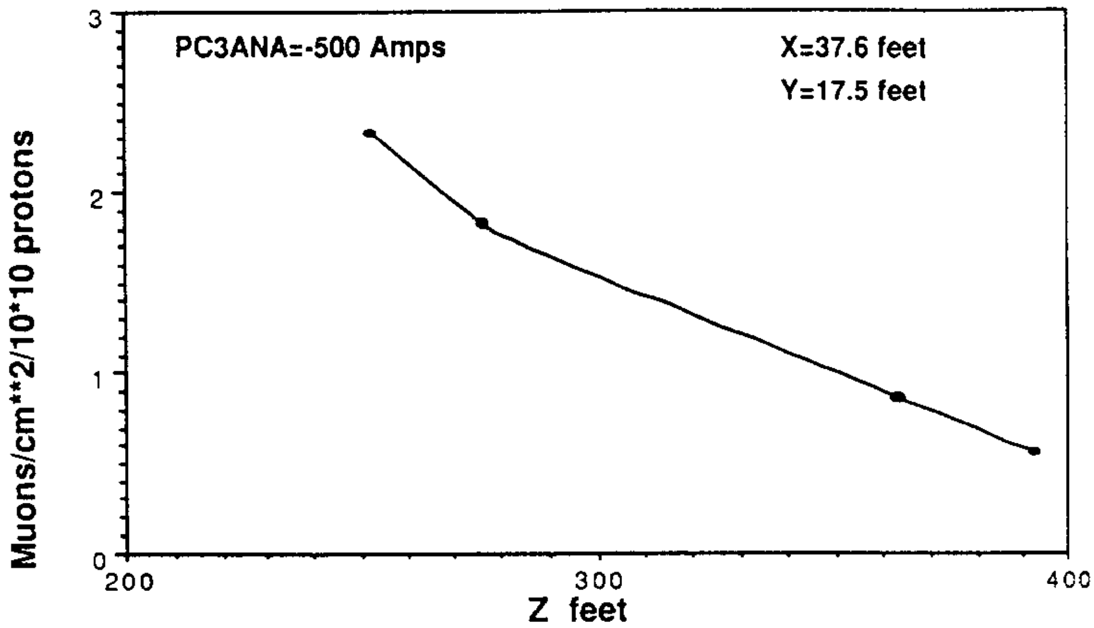

Figure 4 Muon Fluence in Portakamps

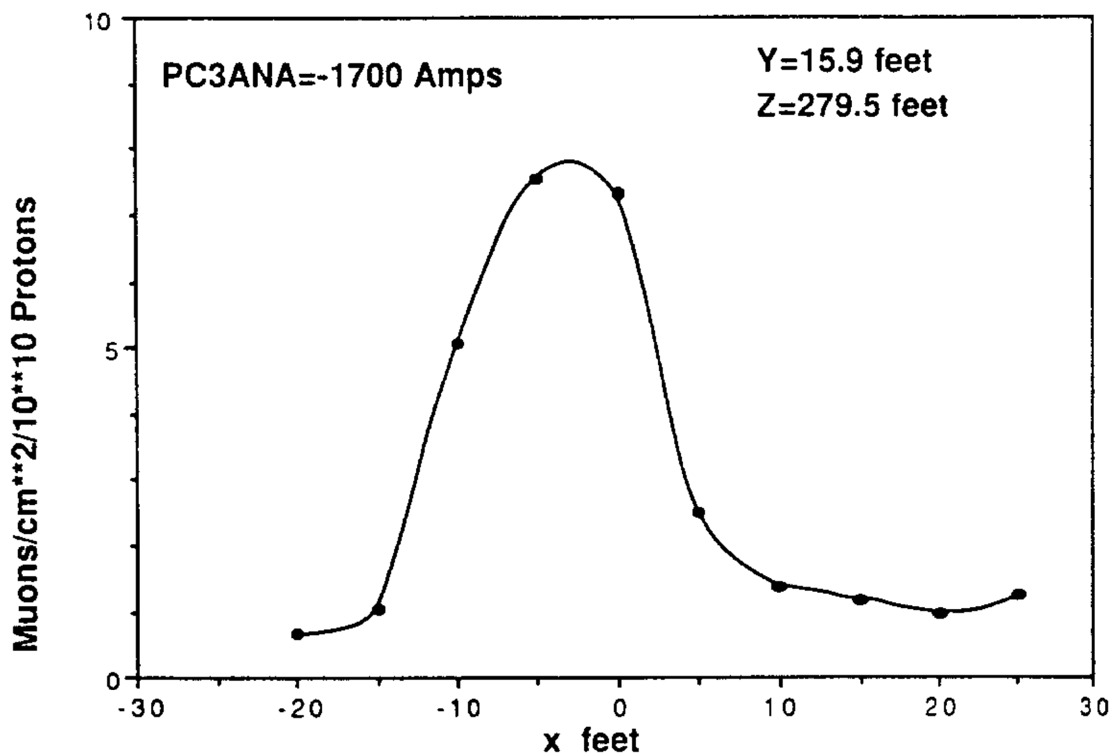

Figure 5 Muon Fluence at Pass A

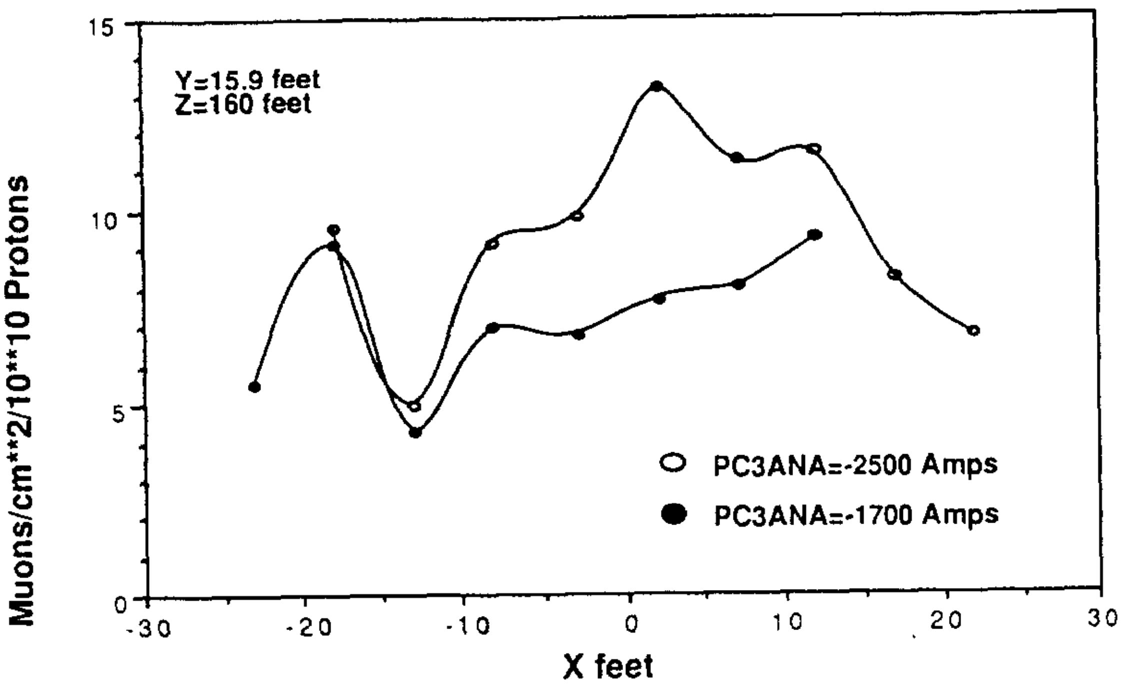

Figure 6 Muon Fluence at Pass B

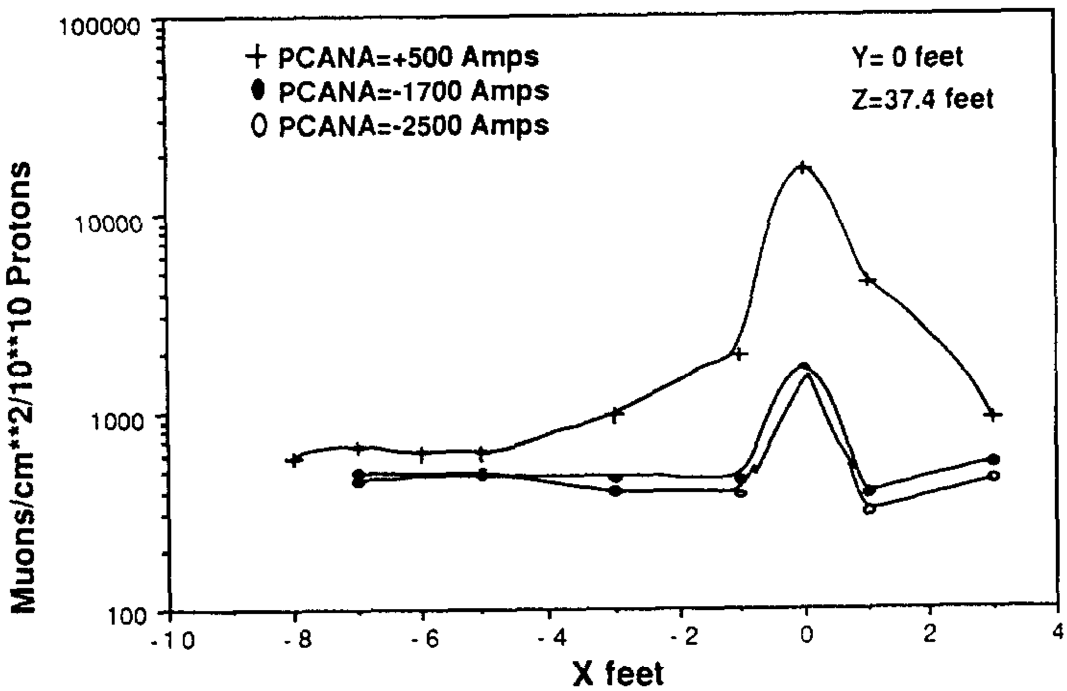

Figure 7 Muon Fluence at Pass C

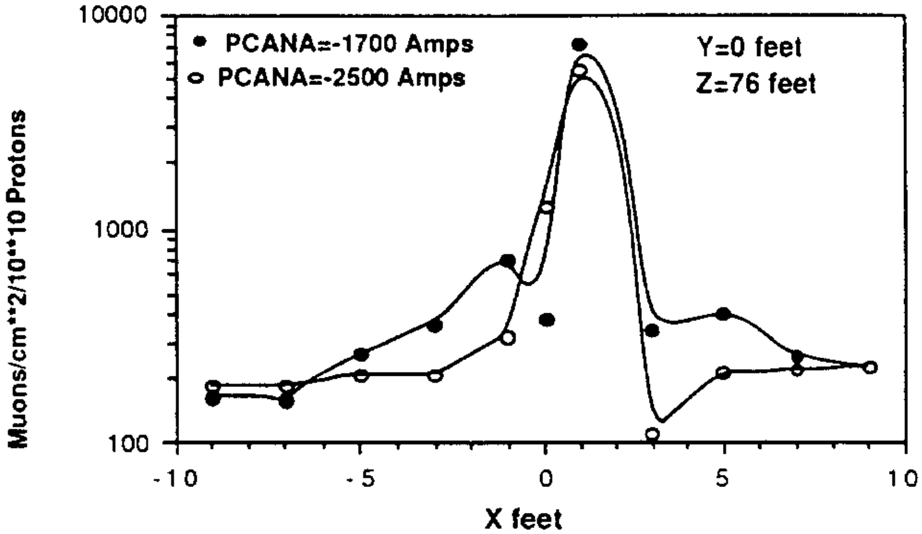

Figure 8 Muon Fluence at Pass D

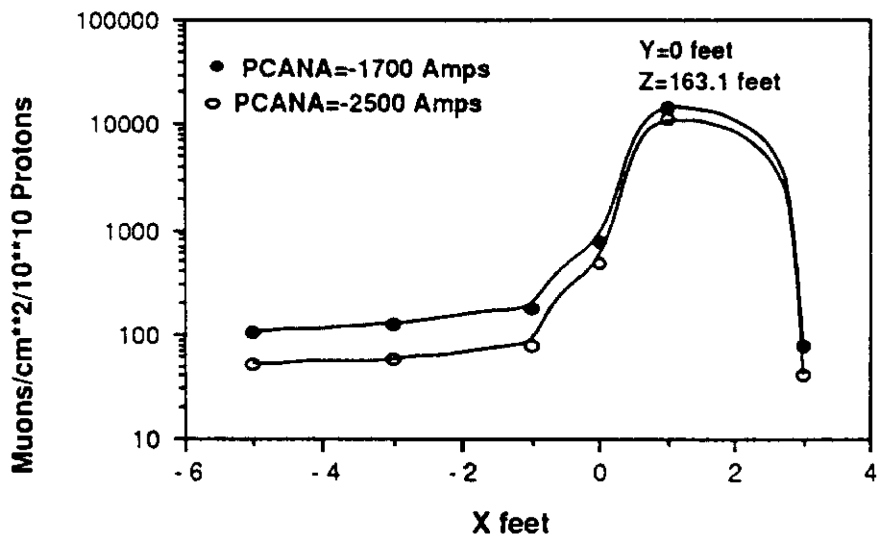

Figure 9 Muon Fluence at Pass E

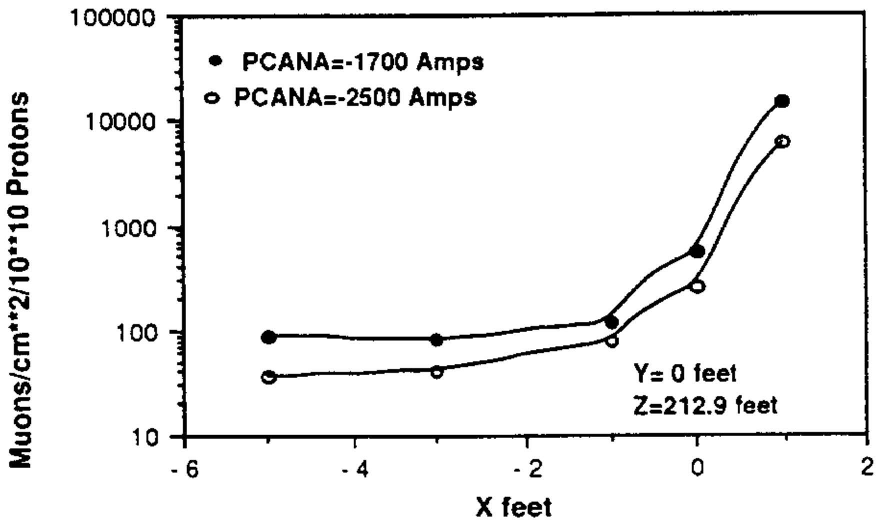

Figure 10 Muon Fluence at Pass F